Bull Yamaguchi Med Sch 46(1-2) : 1-13, 1999

Magnetic Resonance (MR) Imaging of Cranial Nerves in the Cavernous Sinus – with Emphasis on their Correlation with Anatomical Findings and Appropriate Slice Selections for Imaging –

Shoichi Kato

Department of Neurosurgery, Yamaguchi University School of Medicine, 1144 Kogushi, Ube, Yamaguchi, 755-8505, Japan.
(Received December 16, 1998, revised March 5, 1999)

Abstract The purpose of this work was to assess the correlation of magnetic resonance (MR) imaging and anatomic features in depicting the compartments of the cavernous sinus, and to obtain an appropriate MR slice direction for revealing cranial nerves. Thirty-nine cavernous sinuses in human cadavers were examined macroscopically and another 14 cavernous sinuses in human cadavers were studied using 1.5-T MR system. In the macroscopic study, the angle between the anteroposterior line on the tuberculum sellae and the long axis of the nerves was measured. The oculomotor nerve extended downward (16.0 degrees) and laterally (15.5 degrees) from the anteroposterior line. The ophthalmic nerve went upward (8.8 degrees) and slightly laterally (0.7 degrees). The maxillary nerve extended downward (24.7 degrees) and laterally (4.3 degrees). In the MR images using slices matching the direction of each cranial nerve, oblique sagittal images detected the longitudinal courses of the oculomotor (64.3%), ophthalmic (64.3%) and maxillary (71.4%) nerves, and oblique transverse images demonstrated that of oculomotor (64.3%), ophthalmic (71.4%) and maxillary (78.5%) nerves. MR coronal images 1-mm-thick depicted the positions of the oculomotor (100%), trochlear (71.4%), ophthalmic (100%), maxillary (100%) and abducens (85.7%) nerves. MR imaging depicts well the anatomical courses of the nerves, and an appropriate slice is able to demonstrate the long axis of the nerve.

Key words : magnetic resonance imaging, cavernous sinus, cranial nerve, oblique image

Introduction

Magnetic resonance (MR) imaging has become a useful modality for brain imaging, especially in the cranial base[1]. Several studies have demonstrated presence and position of the cranial nerves in the cavernous sinus[2-8]. Depiction of the precise positions and long axes of cranial nerves running in the cavernous sinus on MR images is still unsatisfactory because of their differing courses. Therefore it is useful and important to obtain appropriate slice directions for visualization of these nerves by MR imaging, which is able to obtain variable directed slice images without any bone artifacts. There has been no previous description of the slice direction for MR imaging in the literature. Therefore, the purpose of the present study was to detect the precise course of the cranial nerves located in the cavernous sinus of cadavers macroscopically, and to apply an appropriate slice setting for depicting each of the nerves on MR images. The precise slice direction of MR imaging would be applied in clinical cases.

Materials and Methods

Thirty-nine cavernous sinuses in human cadavers, aged between 56 and 96 years (mean, 79.5 years), were dissected to examine the entrance point, diameter of cranial nerves of the oculomotor, trochlear, trigeminal and abducens nerves, the relation of the course of each cranial nerve, and the direction of each cranial nerve along its long axis. In this study, the basal line was as follows: anteroposterior (Y) direction, parallel to the tuberculum sellae and the lateral (X) and vertical (Z) direction, meeting at right angles with line Y (Fig. 1). Zero point was the middle point between the bilateral posterior clinoid processes. The direction was indicated by measuring the angle between line Y and the long axis of each nerve from the top and lateral views.

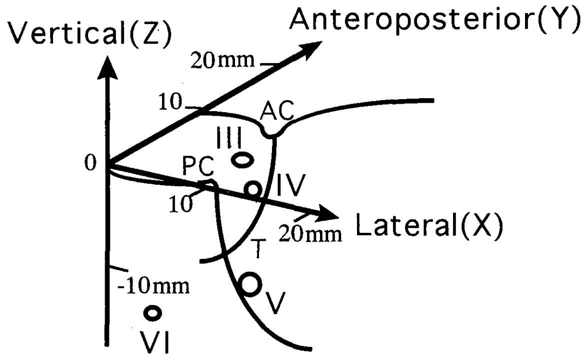

Fig. 1 Basal line measuring the distance of each cranial nerve of the cavernous sinus. Zero point is the middle point of the bilateral posterior clinoid processes. The anteroposterior line (Y) is parallel to the tuberculum sellae on the midsagittal plane. The vertical (Z) and lateral (X) lines are perpendicular to the anteroposterior line through the zero point. The arrow indicates the plus direction for each direction. The circle indicates the entrance point of each cranial nerve. Note.-III= oculomotor nerve; IV= trochlear nerve; V = trigeminal nerve; VI= abducens nerve; AC= anterior clinoid process; PC = posterior clinoid process; T = cerebellar tentorium.

Another 14 cavernous sinuses in human cadavers, aged between 61 and 92 years (mean, 76.2 years), were examined with a 1.5-T superconductive system (Magnetom H15, Siemens). The use of a small-field-of-view coil allowed precise imaging of small sized specimens. T1-weighted spin-echo images were obtained with a repetition time of 600 ms and an echo time of 25 ms. Other parameters were as follows: field of view, 120 to 150 mm ; number of excitations, 3 or 4; matrix, 256 x 256. Serial coronal images parallel to the X-Z plane were obtained at a thickness of 1 or 3 mm. One-millimeter-thick oblique sagittal and oblique transverse sections were also obtained along the course of each cranial nerve, determined by macroscopic examination. Gelatin containing gadopentetate dimeglumine diethylene triamine pentaacetic acid (Gd-DTPA) was injected into the internal carotid artery for delineation of this vessel.

Results

A. Macroscopic study

(1) Entrance point and diameter of nerves

The oculomotor (III), trochlear (IV), ophthalmic (V_1) and maxillary (V_2) nerves coursed inside the lateral wall of the cavernous sinus. The abducens (VI) nerve was the only cranial nerve which traveled through the cavernous sinus. The distance between the basal line and the entrance point of each cranial nerve, where the nerve penetrated the dura, was measured using a three-dimensional approach (Table 1, Fig. 1). The oculomotor and trochlear nerves penetrated the superior wall of the cavernous sinus. The oculomotor nerve entered the cavernous sinus from middle part of the superior wall and the entrance point of the trochlear nerve located in the posterior lateral part of the superior wall of the cavernous sinus beneath the free margin of the cerebellar tentorium. The trigeminal (V) nerve entered Meckel's cave over the apex of petrous bone and lateral to the posterior wall of the cavernous sinus. The abducens nerve entered the cavernous sinus from the inferior part of the posterior wall. It penetrated the dura of the clivus and ascended along the clivus within the basilar plexus. It entered into inferior part of the posterior wall of the

Table 1. The distance to the entrance point where the cranial nerve penetrates the dura and the maximum diameter of the each cranial nerve at the middle of the sella turcica.

	III	IV	V	VI
Distance (mm)				
Lateral (X)	11.8(7~15)	14.0(7~17)	17.2(12.5~23.5)	9.6(6.2~13)
Anteroposterior (Y)	2.8(-1.5~6.5)	-7.6(-13.5~-3)	-11.1(-14.5~-7.5)	-11.1(-20~-7.5)
Vertical (Z)	-1.9(-4.5~0)	-2.0(-6~2)	- 9.2(-14.5~-5)	-14.3(-22.5~-8)
			V_1 / V_2	
Diameter (mm)	2.1(1.8~2.7)	0.9(0.6~1.1)	5.4(3.9~8.0) / 5.4(4.0~8.0)	1.4(0.6~2.2)

The basal point was shown in Figure 1. The diameter was measured through the section of the middle of the sella turcica.

cavernous sinus after passing below the petroclinoid ligament and lateral to the dorsal meningeal artery.

After leaving the Gasserian ganglion, the shape of the ophthalmic and maxillary nerves became oval. The maximum diameters of the oculomotor, trochlear, ophthalmic, maxillary and abducens nerves were determined by measuring their diameters through levels of the sella turcica (Table 1). They were 2.1 mm (oculomotor), 0.9 mm (trochlear), 5.4 mm (ophthalmic), 5.4 mm (maxillary) and 1.4 mm (abducens). The trochlear nerve was the smallest, less than 1 mm in diameter, and the first and second divisions of the trigeminal nerve were the largest.

(2) Courses of the nerves

The photograph of the cadaver in Fig. 2 illustrates the courses of the cranial nerves.

Entering the cavernous sinus from the superior wall, the oculomotor nerve ran downward

A.

B.

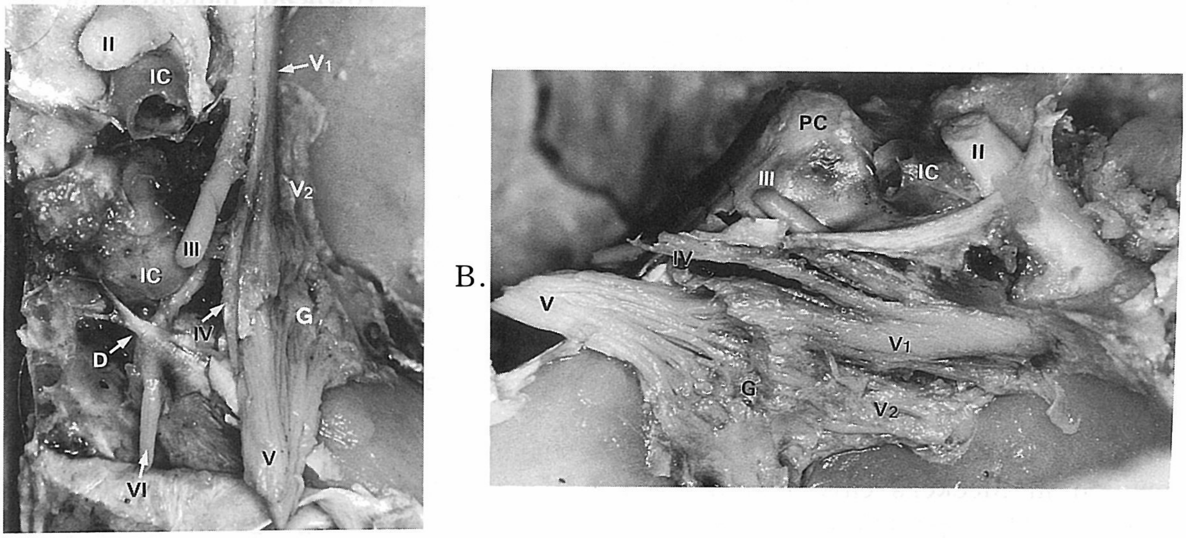

Fig. 2 A, Picture from the top showing the courses of the cranial nerves. The dura and anterior clinoid process are removed. The oculomotor nerve (III) extends laterally. The trochlear nerve (IV) runs above the ophthalmic nerve (V_1). After leaving the Gasserian ganglion (G), the maxillary nerve (V_2) courses more laterally than V_1 Note the abducens nerve (VI) passing through Dorello's canal (D) and running around the internal carotid artery (IC) medial to the Gasserian ganglion. Note. - II = optic nerve.

B, Picture from the lateral view disclosing the courses of the cranial nerves running within the sinus. The lateral wall of the sinus and the anterior clinoid process are removed. The cranial nerves III, IV and V_2 extend downward, whereas V_1 ascends to enter the superior orbital fissure. Note. - PC= posterior clinoid process.

Table 2. The position of the trochlear nerve with correlation to the oculomotor nerve and ophthalmic nerve and its corresponding coronal image through the middle of the sella turcica.

	No.	Type A	Type B	Type C
Macroscopic study	34	14 (41.2%)	4 (11.8%)	16 (47.0%)
MRI study	10	3 (30.0%)	1 (10.0%)	6 (60.0%)

Type A : The trochlear nerve ran beneath the oculomotor nerve.
Type B : The trochlear nerve ran middle point between the oculomotor and ophthalmic nerve.
Type C : The trochlear nerve ran just above the ophthalmic nerve.

and laterally along the upper inside of the lateral wall at levels of the sella turcica. Then it traveled below the anterior clinoid process, finally entering the superior orbital fissure.

The trochlear nerve, after piercing the dura beneath the free margin of the cerebellar tentorium, coursed forward within the lateral wall and met the ophthalmic nerve. After meeting the ophthalmic nerve which proceeded upward, the trochlear nerve changed the course to upwards along the ophthalmic nerve and finally they located over the oculomotor nerve at the anterior portion of the cavernous sinus over the annulus of Zinn and below the orbital periosteum (Fig. 2). Its course was classified into three types with its positional relationship to other nerves through the middle of the sella turcica (Fig. 3). In type A, accounting for 41.2% of all cases, the nerve ran beneath the oculomotor nerve (Table 2, Fig. 3). In type B, accounting for 11.8% of cases, it ran through the middle part between the oculomotor and ophthalmic nerves (Table 2, Fig. 3). In type C, accounting for 47.0% of cases, it extended along and just above the ophthalmic nerve (Table 2, Fig. 3).

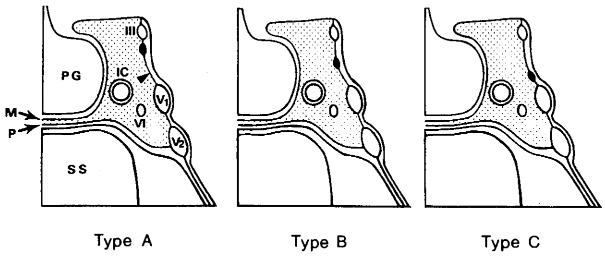

Fig. 3 Three types of courses of the trochlear nerve (solid circle) on coronal sections. Type A : The trochlear nerve runs beneath the oculomotor nerve. An arrowhead indicates the inner layer. Type B : The trochlear nerve runs middle point between the oculomotor and ophthalmic nerve. Type C : The trochlear nerve runs just above the ophthalmic nerve. Note.- III = oculomotor nerve; V_1 = ophthalmic nerve; V_2 = maxillary nerve; VI = abducens nerve; IC = internal carotid artery; M = meningeal layer; P = periosteal layer; PG = pituitary gland ; SS = sphenoid sinus.

The trigeminal nerve formed the Gasserian ganglion in Meckel's cave and had three branches. The ophthalmic and maxillary nerves ran through the lateral wall of the cavernous sinus. After leaving the Gasserian ganglion, the ophthalmic nerve ran forward in an upward direction and slanted slightly laterally into the superior orbital fissure (Fig. 2). The maxillary nerve ran downward and slightly laterally into the foramen rotundum (Fig. 2). These courses were relatively uniform.

The abducens nerve, after ascending the basilar plexus, turned laterally to pass through Dorello's canal, and coursed around the internal carotid artery. It was confined in the narrow space between the carotid artery and the Gasserian ganglion (Fig. 2). Then it coursed forward within the cavernous sinus just lateral to the carotid artery, and came close to the ophthalmic nerve. As the abducens nerve ran very closely to the internal carotid artery, the abducens nerve was displaced when the internal carotid artery was tortuous. On the basis of the relation to the carotid artery, three types of abducens nerve position were recognized (Table 3, Fig. 4). In type 1 (82.0%), there was no contact between these components. In type 2 (2.6%), the abducens nerve was attached laterally to the

Table 3. The position of the abducens nerve with correlation to the internal carotid artery and its corresponding coronal image through the middle of the sella turcica.

	No.	Type 1	Type 2	Type 3
Macroscopic study	39	32 (82.0%)	1 (2.6%)	6 (15.4%)
MRI study	12	10 (83.3%)	0 (0.0%)	2 (16.7%)

Type 1 : The abducens nerve had no contact with the internal carotid artery.
Type 2 : The abducens nerve was attached laterally to the internal carotid artery.
Type 3 : The abducens nerve was attached inferolaterally to the internal carotid artery.

internal carotid artery. In type 3 (15.4%), its inferolateral attachment to the carotid artery was evident.

(3) Directions of the nerves

The directions of the nerves were then examined. The oculomotor, ophthalmic, and maxillary nerves had relatively uniform courses. The angle between the anteroposterior (Y) line and the long axis of each nerve was measured from the top and lateral views (Table 4, Fig. 5). The long axis of ophthalmic and maxillary nerves were indicated by the lines from the center of the Gasserian ganglion to the superior orbital fissure (ophthalmic) and to the foramen rotundum (maxillary). From the top view, these nerves slanted laterally (Fig. 5A). The oblique sagittal angle, which was formed between the midsagittal plane (Y-Z plane) and each nerve, was measured. This angle for the oculomotor, ophthalmic and maxillary nerves was 15.5, 0.7, and 4.3 degrees, respectively (Table 4). From the lateral view (Fig. 5B), the oculomotor and maxillary nerves went downwards, whereas the ophthalmic nerve extended upwards. The oblique transverse angle, which was the angle between the transverse plane (X-Y plane) and each nerve, was also measured. This angle for the oculomotor, ophthalmic and maxillary nerves was 16.0, -8.8, 24.7 degrees, respectively (Table 4). Measurement of the angle for the trochlear and abducens nerves was difficult because of their variable courses, as mentioned above.

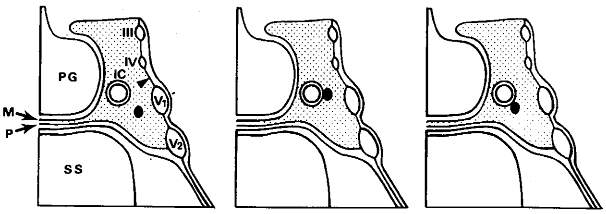

Type 1 Type 2 Type 3

Fig. 4 Three types of relations between the abducens nerve (closed circle) and the internal carotid artery (IC) on the coronal section. Type 1 : The abducens nerve have no contact with the internal carotid artery. An arrowhead indicates the inner layer. Type 2 : The abducens nerve is attached laterally to the internal carotid artery. Type 3 : The abducens nerve is attached inferolaterally to the internal carotid artery. Note.- III = the oculomotor nerve ; IV = the trochlear nerve ; V_1 = the ophthalmic nerve; V_2 = the maxillary nerve ; M = meningeal layer ; P = periosteal layer ; PG = pituitary gland ; SS = sphenoid sinus.

Table 4. The angle between the basal plane and the direction of each cranial nerve by macroscopic study (degrees).

	III	V_1	V_2
from sagittal (Y-Z) plane	α =15.5 (10~20)	β = 0.7 (-3~5)*	γ = 4.3 (-2~12)*
from transverse (X-Y) plane	a =16.0 (8~24)	b =-8.8 (-2.0~-3)**	c =24.7 (14~35)

The angles were shown in Figure 5. * : A minus sign indicated medial inclination. ** : A minus sign indicated upward inclination.

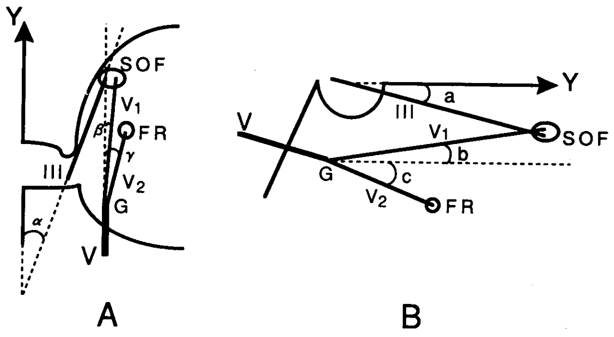

Fig 5. A, Oblique sagittal angle of inclination between the anteroposterior (Y) line and each of the nerves as viewed from the top. The dashed line is parallel to line Y. The angles α, β, and γ correspond to those of the oculomotor (III), ophthalmic (V_1), and maxillary (V_2) nerves. Note. - FR = foramen rotundum ; G = center of the Gasserian ganglion ; SOF = superior orbital fissure ; V= trigeminal nerve.
B, Oblique transverse angle indicating the angle between line Y and the nerves viewed from the lateral. The dashed line is parallel to line Y. The angles a, b and c, correspond those of III, V_1 and V_2.

B. MR imaging study

Fourteen cavernous sinuses in human cadavers were studied using T1-weighted spin-echo imaging, and also specific sections (oblique sagittal and oblique transverse images) were obtained based on the anatomical study mentioned above.

(1) Coronal images

(a) Detection rate

On coronal images sliced through the middle of the sella turcica, the detection rates were compared between slice thicknesses of 1 mm and 3 mm. On coronal slices 3 mm thick, the detection rates for the oculomotor, trochlear, ophthalmic, maxillary and abducens nerves were 92.9%, 42.9%, 100%, 100% and 71.4%, respectively (Table 5), whereas on coronal slices 1 mm thick, the corresponding rates were 100% (oculomotor), 71.4% (trochlear), 100% (ophthalmic), 100% (maxillary) and 85.7% (abducens), respectively (Table 5). Thus the use of thin slices improved the detection rate, especially for small-diameter cranial nerves such as the trochlear and abducens nerves (Fig. 6).

(b) Position of the trochlear nerve

On 10 sides, the trochlear nerve was detected (Table 5), and its positions were examined. The trochlear nerve ran various courses in the lateral wall of the cavernous sinus, as found in the anatomical study. Its course was classifiable into three types on coronal slices taken through the middle of the sella turcica. From the MR images, types A, B, and C were present in 30.0%, 10.0%, and 60.0% of cases, respectively (Table 2), thus coinciding with the anatomical results.

(c) Position of the abducens nerve

The abducens nerve was classified into three types according to its relation to the internal carotid artery on coronal slices through the middle of the sella turcica. On 12 sides detected on coronal images, types 1, 2, and 3 accounted for 83.3%, 0.0% and 16.7% of cases, respectively (Tables 3, 5).

(2) Oblique sagittal and transverse images

In order to detect the long axis of the nerves, oblique sagittal and oblique transverse slices were obtained, according to the angles obtained in the anatomical study, using 1-mm-thick T1-weighted spin-echo images. For the oblique sagittal images of the oculomotor, ophthalmic and maxillary nerves, slanting images were obtained at angles of 15.5, 0.7, and 4.3 degrees from the midsagittal plane (Y-Z plane), respectively (Table 4, Fig. 7A, C, E). These images demonstrated long nerve courses: the oculomotor

Table 5. The detective rate for each cranial nerve on coronal scan in different thickness on MR image.

Thickness	No.	III	IV	V_1	V_2	VI
3 mm	14	13 (92.9%)	6 (42.9%)	14 (100%)	14 (100%)	10 (71.4%)
1 mm	14	14 (100%)	10 (71.4%)	14 (100%)	14 (100%)	12 (85.7%)

A.

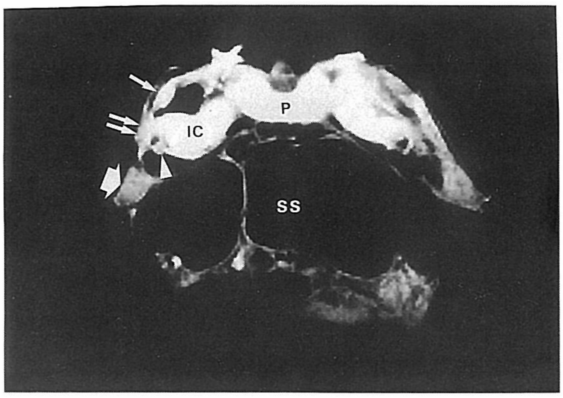

B.

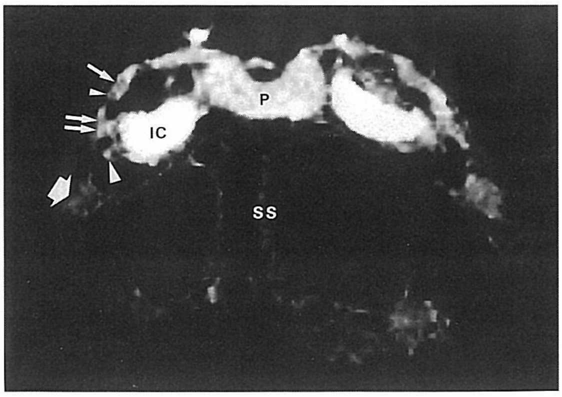

Fig 6. A, A 3-mm-thick coronal section through the middle portion of the sella turcica, showing the oculomotor (small arrow), ophthalmic (double arrows), maxillary (large arrow) and abducens (arrowhead) nerves in the cavernous sinus. The delineation of the trochlear nerve is obscure. Note. - IC = internal carotid artery ; P = pituitary gland ; SS = sphenoid sinus.
B, A 1-mm-thick coronal section of the same specimen through the middle portion of the sella turcica. The oculomotor (small arrow), ophthalmic (double arrows), and maxillary (large arrow) nerves are shown. Note the demonstration of the trochlear nerve (small arrowhead) below the oculomotor nerve. The abducens nerve (large arrowhead) is identifiable just lateral to the internal carotid artery.

Table 6. The detective rate for cranial neve III, V_1 and V_2 using oblique sagittal and oblique transverse section on MR image of 1 mm thickness.

	No.	III	V_1	V_2
Oblique sagittal image	14	9 (64.3%)	9 (64.3%)	10 (71.4%)
Oblique transverse image	14	9 (64.3%)	10 (71.4%)	11 (78.5%)

A.

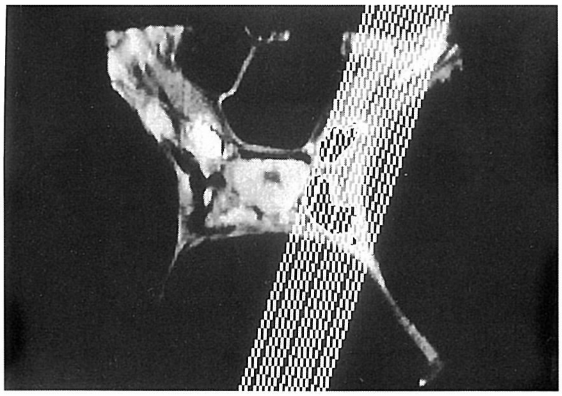

B.

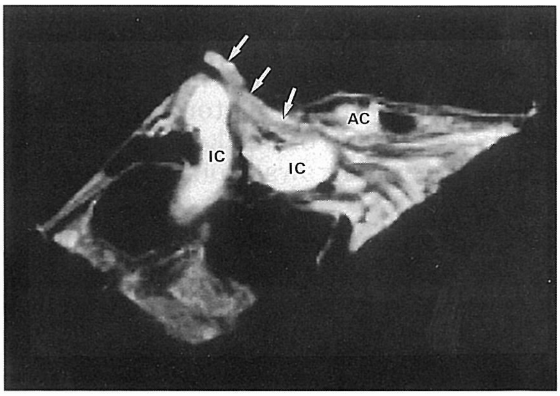

Fig 7. A, A localizer image for oblique sagittal images (15.5 degrees from sagittal plane) of the oculomotor nerve.
B, Oblique sagittal image from A, showing the longitudinal course of the oculomotor nerve (arrows). The oculomotor nerve enters the cavernous sinus from its roof and extends forward and downward below the anterior clinoid process (AC). The cavernous portion of the internal carotid artery (IC) filled with gelatin-gadolinium mixture is also well demonstrated. Note. - SS = sphenoid sinus.

C.

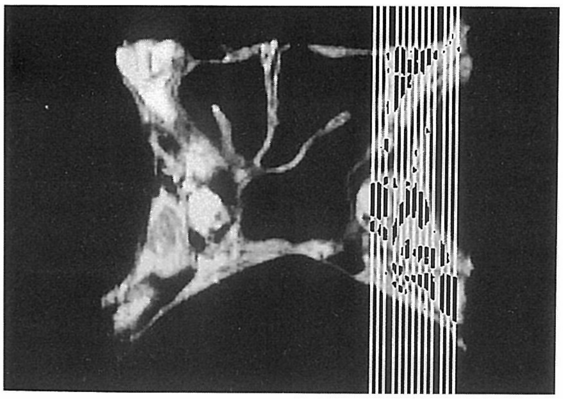

D.

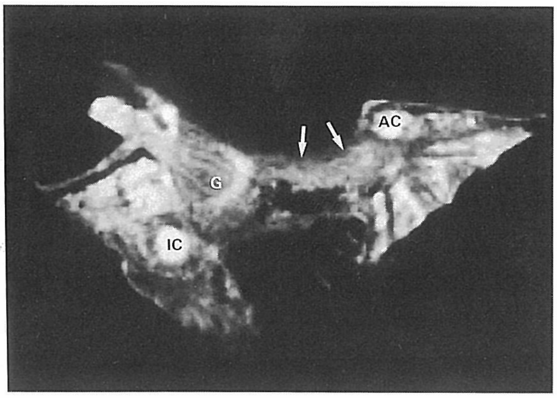

Fig 7. C, A localizer image for the oblique sagittal slices (0.7 degrees from sagittal plane) of the ophthalmic nerve.
D, Oblique sagittal slice obtained from C. The trigeminal root enters the cavernous sinus from a posterior direction above the petrous bone and below the tentorium cerebelli. Gasserian ganglion (G) appears crescent-shaped and its nerve fibers appears sleeve-like. The ophthalmic nerve (arrows) leaves the ganglion and extends forward and upward. The anterior clinoid process (AC) and the petrous portion of the internal carotid artery (IC) containing gelatin-gadolinium mixture are evident.

E.

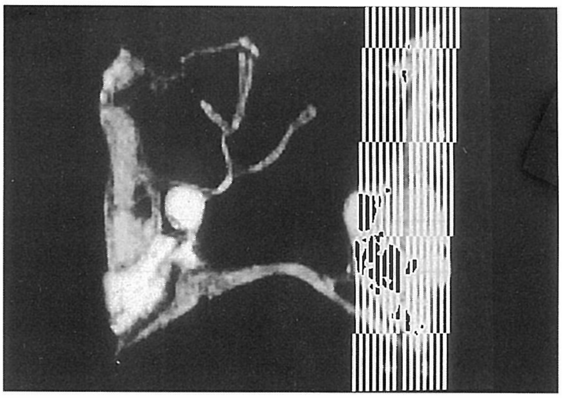

F.

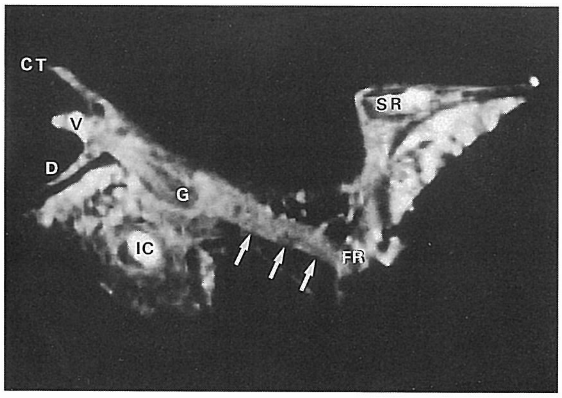

Fig 7. E, A localizer image for the oblique sagittal image (4.3 degrees from sagittal plane) of the maxillary nerve.
F, Oblique sagittal image from E. The trigeminal nerve (V) pierces the dura (D) below the cerebellar tentorium (CT). The oval-shaped Gasserian ganglion (G) is located in the region of Meckel's cave, just above the internal carotid artery (IC). The maxillary nerve (arrows) courses downwards into the foramen rotundum (FR).

nerve extended downwards below the anterior clinoid process (Fig. 7B), and the trigeminal nerve formed the Gasserian ganglion above the internal carotid artery (Fig. 7D, F). After leaving the Gasserian ganglion, upward inclination of the ophthalmic nerve in order to reach the superior orbital fissure, and a downward course of the maxillary nerve into the foramen rotundum were delineated (Fig. 7D, F). The detection rates for the oculomotor, ophthalmic and maxillary nerves were 64.3%, 64.3%, and 71.4%, respectively (Table 6). For the oblique transverse images, angles of 16.0, −8.8, and 24.7 degrees from transverse plane (X-Y plane) were employed for the oculomotor, ophthalmic and maxillary nerve, respectively (Table 4, Fig. 8A, C, E). A minus sign indicates an upward inclination. These images showed the oculomotor and ophthalmic nerves running along the lateral wall, and the maxillary nerve leaving the ganglion to enter the foramen rotundum (Fig. 8B, D, F). The detection rates were 64.3% (oculomotor), 71.4% (ophthalmic) and 78.5% (maxillary) (Table 6). As the trochlear and abducens nerves had small diameters and

A. B.

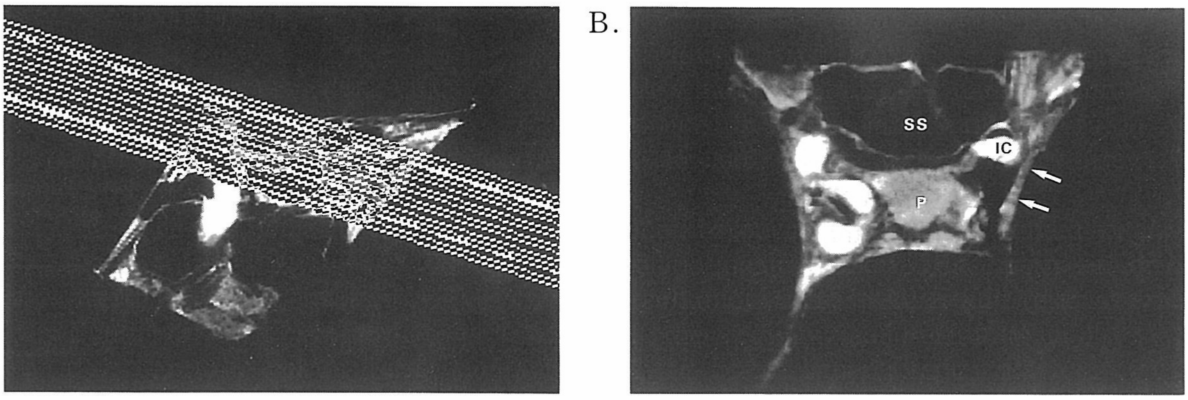

Fig 8. A, A localizer image for an oblique transverse section (16.0 degrees from transverse plane) of the oculomotor nerve.
B, The oculomotor nerve (arrows) is defined on the lateral part of the cavernous sinus. Its longitudinal course is well visualized. The internal carotid artery (IC) and the pituitary gland (P) are demonstrated. Note.-SS = sphenoid sinus.

C. D.

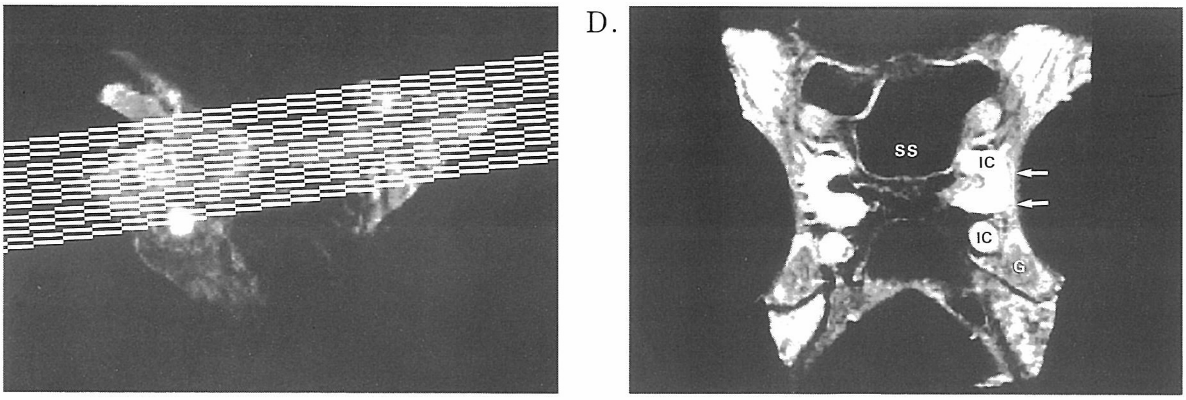

Fig 8. C, A localizer image for the oblique transverse slice (-8.8 degrees from transverse plane) of the ophthalmic nerve.
D, The ophthalmic nerve (arrows) leaves Gasserian ganglion (G) and goes forward along the lateral wall of the sinus. The tortuous internal carotid artery (IC) is delineated as a high signal due to gadolinium injection.

E. F.

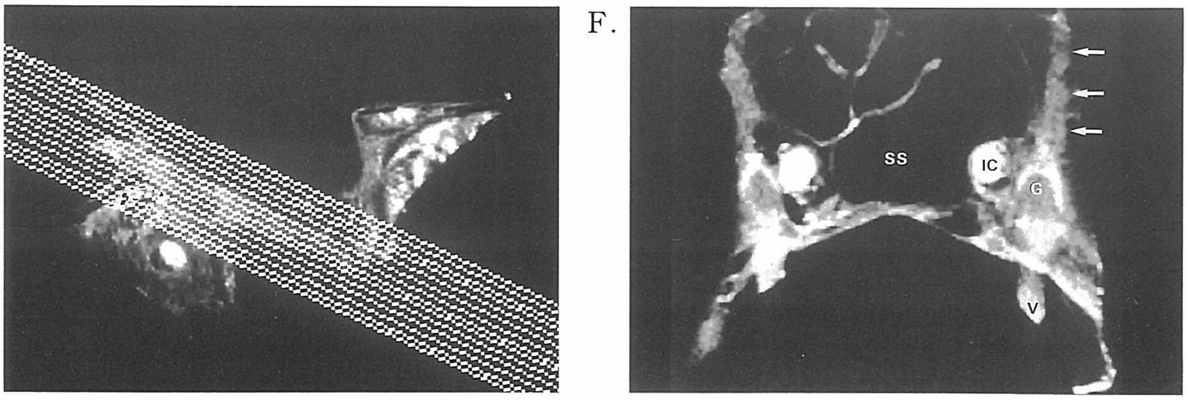

Fig 8. E, A localizer image for the oblique transverse slice (24.7 degrees from transverse plane) of the maxillary nerve.
F, The trigeminal root (V) passes through the cavernous sinus posteriorly and forms the crescent-shaped trigeminal ganglion (G), just lateral to the carotid artery (IC). The maxillary nerve (arrows) runs forward and slightly laterally.

variable courses in the cavernous sinus, it was difficult to visualize their long-axis courses.

Discussion

The cranial nerves in the cavernous sinus have been well studied anatomically and the ability of imaging methods to detect them has been discussed by several authors with reference to CT scan and MR imaging[2,3,9,10]. Most reports have been based on coronal images, but no study has dealt with the precise direction of the variable courses of the nerves. Accurate knowledge of the position and the course of each cranial nerve is of considerable importance for the depiction of the longitudinal course of the cranial nerve on MR images. Therefore in the present study, the most appropriate slice imaging along the longitudinal axis of these nerves was determined on the basis of macroscopic examination.

Macroscopic study

Anatomical studies reported by several authors have provided some information from which to decide the most suitable surgical approach to parasellar lesions and for their diagnosis[9–17]. The cavernous sinus is an area of venous vasculature formed by two layers of the dura (i.e. the meningeal and periosteal layers). The lateral wall consists of outer and inner layers[5,14,16,18]. Bonneville et al.[19] also reported that there is a venous space within the lateral wall of the cavernous sinus. Therefore there may be more than two layers in the lateral wall of the cavernous sinus. The oculomotor and trochlear nerves, and the first and second divisions of the trigeminal nerves, are located in the inner layer of the lateral wall of the cavernous sinus[15,16,18]. The abducens nerve runs within the cavernous sinus after passing through Dorello's canal, which consists of the apex of the petrous bone, the dorsum sellae, and the petroclinoid ligament (or petrosphenoidal ligament of Gruber)[20]. From the present study, the oculomotor and maxillary nerves ran laterally and downwards, whereas the ophthalmic nerve proceeded laterally and upwards. The directions of the nerves differ because their entrance points and exit foramens are different. The entrance point of the oculomotor nerve is the middle of the roof of the cavernous sinus, whereas that of the trigeminal nerve is over the apex of the petrous bone and lateral to the posterior wall of the cavernous sinus[3,21]. The oculomotor, trochlear, ophthalmic, and abducens nerves proceed into the superior orbital fissure, whereas the maxillary nerve enters the foramen rotundum[16]. These anatomical conditions determine the nerve directions and change their relationship. Embedded in the lateral wall of the cavernous sinus, the oculomotor, trochlear, ophthalmic and maxillary nerves were arranged in this order from the uppermost through levels of the sella turcica[9,21].

The internal carotid artery had a tortuous course within the cavernous sinus and its course was also classified by the relationship to the surrounding venous spaces[16]. In our study, the abducens nerves were displaced by the tortuous carotid artery in the type 2 and type 3 groups. The position of the abducens nerve was classified into three types on the basis of the relationship to the carotid artery through the middle of the sella turcica.

The present findings confirm that the nerves have a variable relationship to each other during their course in the cavernous sinus.

MR imaging study

MR imaging offers considerable advantages over CT scan for evaluation of cranial nerves and parasellar lesions[1,4–7]. On coronal images through the middle of the sella turcica, cranial nerves show constant relations to the horizontal segment of the internal carotid artery. The oculomotor nerve is superolateral to this segment of the internal carotid artery and the trochlear nerve is lateral to this segment. The ophthalmic and abducens nerves are inferolateral to this segment of the internal carotid artery[2,22]. From our anatomical results, the oculomotor, ophthalmic and maxillary nerves take a relatively constant course, but the trochlear and abducens nerves take a variable course in the cavernous sinus. A previous report stated that the trochlear nerve could not be separated from the oculomotor nerve in 5-mm-thick coronal T1-weighted images because of its small size and close apposition to the oculomotor nerve[22]. As the cranial nerves were found to have small diameters in the macroscopic study, we used 1-mm-thick slices to avoid a partial volume effect. Our MR study verified that thinner slices were effective for visualizing these small cranial nerves, especially the trochlear and abducens nerves, because of the minimal effect of volume averaging from surrounding venous and membranous structures.

The detection of the small trochlear nerve is important for making decisions about the surgical approach through the lateral wall. Surgically the cavernous sinus can be opened through the space between the oculomotor and trochlear nerves (the space of paramedial triangle), or the space between the trochlear and ophthalmic nerves (the space of Parkinson's triangle)[11,13,14,23]. Deterioration of cranial nerve function after surgical resection of tumors involving the cavernous sinus has been reported[24,25]. Preoperative recognition of these nerves will help to prevent injury to the cranial nerves during surgery.

MR imaging has the additional advantage of allowing selection of the optional slice direction. For revealing the cranial nerves, a specific slice direction was selected. It is well known that the course of the optic nerve runs downward at minus 15 to 20 degrees to the orbito-meatal line. Oblique sagittal imaging demonstrates the relationship between the vasculature and the trigeminal and facial nerves in the cisternal portion in patients with facial spasm and trigeminal neuralgia[26]. In the cavernous sinus, evaluation of the nerves requires appropriate imaging slices. As to the detection of the trigeminal nerves on MR imaging, Daniels et al.[27] laid a stress on importance of the sagittal image in addition to the coronal one. Laine et al.[28] also reported the effectiveness of sagittal images in case of perineural tumor extension through the foramen ovale. In addition, our present study has successfully shown the longitudinal entities of the intracavernous cranial nerves throughout the postero-anterior extent by the appropriate oblique sagittal and oblique transverse sections, further emphasizing the importance of choosing the most suitable slice imaging.

The detection rate for each cranial nerve differs on oblique sagittal and oblique transverse images. The maxillary nerve was detected more frequently than the oculomotor and ophthalmic nerves. The trochlear and abducens nerves were not detected along their longitudinal course on MR images. This difference is due to the nerve diameter[3]. The variable courses of the the trochlear and abducens nerves in the cavernous sinus also make it difficult to obtain their long-axis images[17,20].

Conclusions

T1-weighted 1-mm-thick MR images improved the detection rate for the oculomotor, trochlear and abducens nerves compared to 3-mm-thick MR images. The anatomical study of the cavernous sinus clarified the oblique angles between the axes of the cranial nerves and the sagittal and transverse planes. Oblique sagittal and oblique transverse MR images, taken in directions determined by the oblique angles obtained in anatomical studies, depict well the longitudinal courses of the oculomotor, ophthalmic and maxillary nerves in the cavernous sinus.

Acknowledgments

The author is grateful to Professor Haruhide Ito (Department of Neurosurgery, Yamaguchi University), Professor Reiji Kishida (Department of Anatomy, Yokohama City University School of Medicine), Professor Yun Peng Huang (Department of Radiology, Mount Sinai Medical Center), and Dr. Chun Siang Chen (Department of Neurosurgery, Mount Sinai Medical Center) for their useful advice. The author wishes to thank Yumiko Ueno (Konan Saint Hill Hospital) for her technological assistance.

References

1) Pech, P. : Correlative investigations of craniospinal anatomy and pathology with computed tomography, magnetic resonance imaging and cryomicrotomy. *Acta Radiol Suppl (Stockh)*, **372** : 127-148, 1988.

2) Daniels, D.L., Czervionke, L.F., Bonneville, J.F., Cattin, F., Mark, L.P., Pech,

P., Hendrix, L.E., Smith, D.F., Haughton, V.M. and Williams, A.L. : MR imaging of the cavernous sinus: value of spin echo and gradient recalled echo images. *AJNR*, **9** : 947-952, 1988.

3) Tsuha, M., Aoki, H. and Okamura, T. : Roentgenological investigation of cavernous sinus structure with special reference to paracavernous cranial nerves. *Neuroradiology*, **29** : 462-467, 1987.

4) Gentry, L.R., Mehta, R.C., Appen, R.E. and Weinstein, J.M. : MR imaging of primary trochlear nerve neoplasms. *AJNR*, **12** : 707-713, 1991.

5) El-Kalliny, M., van Loveren, H., Keller, J. T. and Tew, J.M. Jr. : Tumors of the lateral wall of the cavernous sinus. *J. Neurosurg.*, **77** : 508-514, 1992.

6) Hirsch, W.L. Jr., Hryshko, F.G., Sekhar, L.N., Brunberg, J., Kanal, E., Latchaw, R. E. and Curtin, H. : Comparison of MR imaging, CT, and angiography in the evaluation of the enlarged cavernous sinus. *AJR*, **151** : 1015-1023, 1988.

7) Shen, W.C., Yang, D.Y., Ho, W.L., Ho, Y. J. and Lee, S.K. : Neurilemmoma of the oculomotor nerve presenting as an orbital mass : MR findings. *AJNR*, **14** : 1253-1254, 1993.

8) Vogl, T., Dresel, S., Lochmüller, H., Bergman, C., Reimers, C. and Lissner, J. : Third cranial nerve palsy caused by gummatous neurosyphilis: MR findings. *AJNR*, **14** : 1329-1331, 1993.

9) Umansky, F. and Nathan, H. : The lateral wall of the cavernous sinus with special reference to the nerves related to it. *J. Neurosurg.*, **56** : 228-234, 1982.

10) Sekhar, L.N., Burgess, J. and Akin, O. : Anatomical study of the cavernous sinus emphasizing operative approaches and related vascular and neural reconstruction. *Neurosurgery*, **21** : 806-816, 1987.

11) Parkinson, D. : A surgical approach to the cavernous portion of the carotid artery : Anatomical studies and case report. *J. Neurosurg.*, **23** : 474-483, 1965.

12) Bedford, M.A. : The "cavernous sinus". *Brit. J. Ophthal.*, **50** : 41-46, 1966.

13) Dolenc, V. : Direct microsurgical repair of intracavernous vascular lesions. *J. Neurosurg.*, **58** : 824-831, 1983.

14) Hakuba, A., Tanaka, K., Suzuki, T. and Nishimura, S. : A combined orbitozygomatic infratemporal epidural and subdural approach for lesions involving the entire cavernous sinus. *J. Neurosurg.*, **71** : 699-704, 1989.

15) Harris, F.S. and Rhoton, A.L. Jr. : Anatomy of the cavernous sinus : A microsurgical study. *J. Neurosurg.*, **45** : 169-180, 1976.

16) Inoue, T., Rhoton, A.L. Jr., Theele, D. and Barry, M.E. : Surgical approaches to the cavernous sinus : A microsurgical study. *Neurosurgery*, **26** : 903-932, 1990.

17) Lang, J. : *Clinical anatomy of the head, neurocranium, orbit, craniocervical regions*. Springer-Verlag Berlin, Heidelberg, New York, 1983, pp.185-203.

18) Taptas, J.N. : The so-called cavernous sinus : A review of the controversy and its implications for neurosurgeons. *Neurosurgery*, **11** : 712-717, 1982.

19) Bonneville, J.F., Cattin, F., Racle, A., Bouchareb, M., Boulard, D., Potelon, P. and Tang, Y.S. : Dynamic CT of the laterosellar extradural venous spaces. *AJNR*, **10** : 535-542, 1989.

20) Nathan, H., Ouaknine, G. and Kosary, I. Z. : The abducens nerve. Anatomical variations in its course. *J. Neurosurg.*, **41** : 561-566, 1974.

21) Gray, H. and Clemente, C.D. : *Gray's anatomy*, Lea and Febiger, Philadelphia, 1985, pp.1154-1170.

22) Daniels, D.L., Pech, P., Mark, L., Pojunas, K., Williams, A.L. and Haughton, V.M. : Magnetic resonance imaging of the cavernous sinus. *AJNR*, 6 : 187-192, 1985.

23) Dolenc, V.V. : *Anatomy and Surgery of the Cavernous Sinus*. Springer-Verlag, Wien, New York, 1989, pp. 7-35.

24) O'Sullivan, M.G., van Loveren, H.R. and Tew, J.M. Jr. : The surgical resectability of meningiomas of the cavernous sinus. *Neurosurgery*, **40** : 238-247, 1997.

25) Knosp, E., Perneczky, A., Koos, W.T., Fries, G. and Matula, C.: Meningiomas of the space of the cavernous sinus. *Neurosurgery*, **38** : 434-444, 1996.

26) Nagaseki, Y., Horikoshi, T., Omata, T., Ueno, T., Uchida, M., Nukui, H., Tsuji, R. and Sasaki, H. : Oblique sagittal mag-

netic resonance imaging visualizing vascular compression of the trigeminal or facial nerve. *J. Neurosurg.*, **77** : 379-386, 1992.

27) Daniels, D.L., Pech, P., Pojunas, K.W., Kilgore, D.P., Williams, A.L. and Haughton, V.M. : Trigeminal nerve: Anatomic correlation with MR imaging. *Radiology*, **159** : 577-583, 1986.

28) Laine, F.J., Braun, I.F., Jensen, M.E., Nadel, L. and Som, P.M. : Perineural tumor extension through the foramen ovale : Evaluation with MR imaging. *Radiology*, **174** : 65-71, 1990.